THE JOURNAL OF BIOLOGICAL CHEMISTRY VOL. 282, NO. 30, pp. 21953–21961, July 27, 2007

Retinoic Acid-inducible Gene-I and Interferon-β Promoter Stimulator-1 Augment Proapoptotic Responses Following Mammalian Reovirus Infection via Interferon Regulatory Factor-3*[S]

Received for publication, March 12, 2007, and in revised form, May 8, 2007 Published, JBC Papers in Press, May 31, 2007, DOI 10.1074/jbc.M702112200

Geoffrey H. Holm[‡§], Jennifer Zurney[¶1], Vanessa Tumilasci[‖1,2], Simon Leveille[‖], Pranav Danthi[‡§], John Hiscott[‖3], Barbara Sherry[¶], and Terence S. Dermody[‡§‡‡4]**

From the Departments of [‡]Pediatrics and [‡‡]Microbiology and Immunology and the [§]Elizabeth B. Lamb Center for Pediatric Research, Vanderbilt University School of Medicine, Nashville, Tennessee, 37232, the Departments of [¶]Microbiology and [**]Molecular Biomedical Sciences, North Carolina State University, Raleigh, North Carolina 27606, and the [‖]Terry Fox Molecular Oncology Group, Lady Davis Institute for Medical Research, McGill University, Montreal, Quebec H3T 1E2, Canada

During viral infection, cells initiate antiviral responses to contain replication and inhibit virus spread. One protective mechanism involves activation of transcription factors interferon regulatory factor-3 (IRF-3) and NF-κB, resulting in secretion of the antiviral cytokine, interferon-β. Another is induction of apoptosis, killing the host cell before virus disseminates. Mammalian reovirus induces both interferon-β and apoptosis, raising the possibility that both pathways are initiated by a common cellular sensor. We show here that reovirus activates IRF-3 with kinetics that parallel the activation of NF-κB, a known mediator of reovirus-induced apoptosis. Activation of IRF-3 requires functional retinoic acid inducible gene-I and interferon-β promoter stimulator-1, but these intracellular sensors are dispensable for activation of NF-κB. Interferon-β promoter stimulator-1 and IRF-3 are required for efficient apoptosis following reovirus infection, suggesting a common mechanism of antiviral cytokine induction and activation of the cell death response.

A primary function of the innate immune system is to detect nascent viral infections and direct subsequent cellular responses. The innate immune system responds to infection by producing a range of soluble cytokines, such as interferon-β (IFN-β),[5] that create an antiviral state in surrounding tissue. In response to these immune pressures, viruses have evolved multiple strategies for subverting innate immunity, which frequently center on manipulating cell death pathways. The interface between the innate immune response, viral infection, and the cellular apoptotic machinery is therefore a critical nexus of disease pathogenesis.

Cells possess a variety of sensors to detect invading pathogens. Toll-like receptors (TLRs) and other pattern recognition receptors, including the nucleotide-binding oligomerization domain proteins and RNA helicases such as retinoic acid-inducible gene-I (RIG-I) and melanoma differentiation-associated protein-5 (Mda-5), recognize viral pathogen-associated molecular patterns (1). TLRs are expressed on the cell surface and recognize extracellular pathogen-associated molecular patterns, whereas RIG-I and Mda-5 detect intracellular viral RNA products (2–4). RIG-I recognizes viral RNAs from the *Flaviviridae*, *Orthomyxoviridae*, *Paramyxoviridae*, and *Rhabdoviridae* families, whereas Mda-5 is involved in the response to *Picornaviridae* (4). The ligand for RIG-I has been identified as a 5′ triphosphate moiety on single- or double-stranded RNA (5, 6); the molecular ligand for Mda-5 is unknown. Following ligand engagement, these intracellular sensors signal through caspase activation and recruitment domains to activate the adaptor, interferon-β promoter stimulator-1 (IPS-1/MAVS/VISA/Cardif) (7–10). IPS-1 activates inhibitor of κB kinase (IKK)-α, IKK-β, IKK-ε, and Tank-binding kinase 1 to phosphorylate transcription factors, including activating transcription factor-2/c-Jun, NF-κB, and interferon regulatory factor-3 (IRF-3), which direct transcription of antiviral genes.

The main cytokine effectors of the innate antiviral response are type I interferons IFN-α and IFN-β, which are secreted

* This work was supported by Public Health Service Awards T32 AI49824 and F32 AI071440 (to G. H. H.), R01 AI50080 (to T. S. D.), and R01 AI62657 (to B. S.), by the Elizabeth B. Lamb Center for Pediatric Research, and by grants from the Canadian Institutes of Health Research, the National Cancer Institute of Canada, the Canadian Cancer Society, and the Terry Fox Program (to J. H.). Additional support was provided by Public Health Service awards P30 CA68485 for the Vanderbilt-Ingram Cancer Center and P60 DK20593 for the Vanderbilt Diabetes Research and Training Center. The costs of publication of this article were defrayed in part by the payment of page charges. This article must therefore be hereby marked "*advertisement*" in accordance with 18 U.S.C. Section 1734 solely to indicate this fact.

[S] The on-line version of this article (available at http://www.jbc.org) contains supplemental text and supplemental Figs. S1–S7.

[1] These authors contributed equally to this work.

[2] Supported by a National Sciences and Engineering Research Council of Canada Studentship award.

[3] Supported by a Canadian Institutes of Health Research senior investigator award.

[4] To whom correspondence should be addressed: Vanderbilt University School of Medicine, D7235 Medical Center North, 1161 21st Ave. South, Nashville, TN 37232-2581. Tel.: 615-343-9943; Fax: 615-343-9723; E-mail: terry.dermody@vanderbilt.edu.

[5] The abbreviations used are: IFN, interferon; TLR, Toll-like receptor; RIG-I, retinoic acid inducible gene-I; Mda-5, melanoma differentiation-associated protein-5; IPS-1, interferon-β promoter stimulator-1; IKK, inhibitor of κB kinase; IRF-3, interferon regulatory factor-3; ISG, interferon-stimulated gene; PKR, protein kinase R; ds, double-stranded; MEF, mouse embryo fibroblast; T3D, type 3 Dearing; ISVP, infectious subvirion particle; STAT, signal transducers and activators of transcription; MOI, muliplicity of infection; PFU, plaque-forming unit(s); PBS, phosphate-buffered saline; RT, reverse transcription; siRNA, small interfering RNA.

from cells and act in an autocrine or paracrine manner via binding to a common IFN-α/β receptor (11). Receptor engagement activates the JAK/STAT signaling pathway, which initiates a second transcriptional response to induce IFN-stimulated genes (ISGs), which directly mediate antiviral effects. One such ISG is IRF-7, which enhances IFN production (12). Other ISGs, such as 2′,5′-oligoadenylate synthase, RNase L, and protein kinase R (PKR), inhibit cellular protein synthesis to prevent viral replication (11).

Innate antiviral responses interface both directly and indirectly with the cellular apoptosis machinery. Type I IFNs mediate proapoptotic responses, as several ISGs have ascribed functions in both extrinsic and intrinsic pathways of apoptosis (11). Proapoptotic ISGs include tumor necrosis factor-related apoptosis-inducing ligand (13) and Fas (14). However, these effects may be cell type- or context-dependent (11). Innate immune signaling also may induce apoptotic cell death in an IFN-independent manner. IPS-1 localizes to the outer membrane of mitochondria, suggesting that it coordinates the antiviral response with pro- or antiapoptotic Bcl-2 family members (8). IPS-1 also associates with Fas-associated via death domain (FADD) to mediate NF-κB activation (7), suggesting that Fas-associated via death domain (FADD) may link activation of RIG-I and Mda-5 to extrinsic apoptotic pathways. Finally, activation of IRF-3 may directly induce apoptosis via a mechanism independent of its induction of IFN (15). Therefore, pathogen detection mechanisms are hardwired into the cellular apoptotic response.

Mammalian reoviruses are nonenveloped viruses with a genome of 10 segments of double-stranded (ds) RNA (16). Following infection of newborn mice, reovirus disseminates to the central nervous system, heart, and liver (17). Apoptosis induced by reovirus is the primary mechanism for virus-induced encephalitis (18) and myocarditis (19). NF-κB plays an important regulatory role in apoptosis evoked by reovirus in cultured cells (20) and *in vivo* (21).

Reovirus induces IFN-β in cultured cells and in infected animals. In the heart, IFN-β is protective (21), and reovirus induction of and sensitivity to IFN-β in cardiac myocytes correlates with the capacity of a given strain to cause myocarditis (21, 22). IFN-β levels induced by reovirus differ in cardiac myocytes and cardiac fibroblasts (23), suggesting that mechanisms of reovirus-induced IFN-β production are also cell type-specific. IRF-3 is required for IFN-β induction following reovirus infection of cardiac myocytes (24). However, mechanisms of reovirus-induced IRF-3 activation are unknown.

To better understand mechanisms of reovirus-induced IFN production and the interface between these pathways and apoptosis, we conducted experiments to identify the viral and cellular determinants of IFN production following reovirus infection and the functional role of these pathways in reovirus replication and apoptosis induction. The results demonstrate that reovirus activates IRF-3 via a mechanism dependent on virion disassembly in endosomes, viral genomic dsRNA, RIG-I, and IPS-1. In contrast, RIG-I and IPS-1 are dispensable for reovirus-induced activation of NF-κB. IRF-3 limits reovirus spread in culture, in part because of production of type 1 IFNs. Importantly, IRF-3 and IPS-1 are required for efficient induction of apoptosis following reovirus infection. These results indicate that RIG-I and IPS-1 are involved in cell death signaling responses to viral infection and provide a functional link between innate immune activation and apoptosis.

EXPERIMENTAL PROCEDURES

Cells, Viruses, and Reagents—HeLa cells, 293T cells, and mouse embryo fibroblasts (MEFs) were maintained in Dulbecco's modified Eagle's medium supplemented to contain 10% fetal bovine serum, 2 mM L-glutamine, 100 units/ml of penicillin, 100 μg/ml streptomycin, and 25 ng/ml of amphotericin B (Invitrogen). L929 cells were maintained in Joklik's minimum essential medium supplemented to contain 10% fetal bovine serum, 2 mM L-glutamine, 100 units/ml of penicillin, 100 μg/ml streptomycin, and 25 ng/ml of amphotericin B. MEFs deficient in IRF-3 (25) were obtained from Dr. Karen Mossman.

Reovirus strain type 3 Dearing (T3D) is a laboratory stock. Reovirus rsT3D-σ1T249I was recovered by plasmid rescue and is isogenic to T3D with the exception of a single amino acid substitution in the σ1 protein rendering it insensitive to protease cleavage and therefore capable of generating infectious subvirion particles (ISVPs) with infectivity equivalent to that of T3D virions (26). Purified reovirus virions were generated using second or third passage L-cell lysates stocks of twice plaque-purified reovirus as described (27). Viral particles were Freon-extracted from infected cell lysates, layered onto 1.2–1.4-g/cm^3 CsCl gradients, and centrifuged at 62,000 $\times$ *g* for 18 h. Bands corresponding to virions (1.36 g/cm^3) and genome-deficient particles (1.29 g/cm^3) (28) were collected and dialyzed in virion storage buffer (150 mM NaCl, 15 mM $MgCl_2$, 10 mM Tris-HCl, pH 7.4). Concentrations of reovirus virions in purified preparations were determined from an equivalence of 1 OD unit at 260 nm equals 2.1×10^{12} virions (28). Viral titer was determined by plaque assay using murine L929 cells (29). ISVPs were generated as described (30) and confirmed by SDS-PAGE and Coomassie Brilliant Blue staining.

Rabbit antisera specific for IRF-3 and IRF-7 were purchased from Santa Cruz Biotechnology (Santa Cruz, CA). Fluorescently conjugated secondary antibodies were purchased from Molecular Probes (Invitrogen). Plasmid p-55C1BLuc (31) was obtained from Dr. T. Fujita. Plasmids pRenilla-Luc and pNF-κB-Luc were obtained from Dr. Dean Ballard (32). siRNA specific for IPS-1 was purchased from Dharmacon (Lafayette, CO), and siRNAs specific for RIG-I and Mda-5 were purchased from Invitrogen. Recombinant mouse IFN-β was purchased from Calbiochem.

Immunoblot Assay—HeLa cells (8×10^5) were either adsorbed with T3D at an MOI of 100 PFU/cell or mock infected in serum-free medium at 4 °C for 1 h, followed by incubation in serum-containing medium at 37 °C for various intervals. Nuclear extracts were prepared as described previously (33). Extracts (10 μg of total protein) were resolved by electrophoresis in 4–20% polyacrylamide gels and transferred to nitrocellulose membranes. Native PAGE for detecting IRF-3 dimers was performed as described (34). The membranes were blocked at 4 °C overnight in blocking buffer (PBS containing 0.5% Tween 20) and incubated with primary antibodies diluted 1:200 to

1:500 in blocking buffer at room temperature for 1 h. The membranes were washed three times for 10 min each with washing buffer (PBS containing 0.5% Tween 20) and incubated with horseradish peroxidase-conjugated goat anti-rabbit (Amersham Biosciences) diluted 1:2000. Following three washes, the membranes were incubated for 1 min with chemiluminescent peroxidase substrate (Amersham Biosciences) and exposed to film.

Indirect Immunofluorescence—HeLa cells (5×10^4) were seeded onto glass coverslips in 24-well plates (Costar, Cambridge, MA). The cells were either adsorbed with T3D at an MOI of 100 PFU/cell or mock infected in serum-free medium at 4 °C for 1 h, followed by incubation in serum-containing medium at 37 °C for 8 h. The cells were fixed with methanol at −20 °C for at least 30 min and incubated with 5% bovine serum albumin (in PBS) for 15 min, followed by incubation with rabbit anti-IRF-3 antiserum (1:50) in PBS containing 0.5% Triton X-100 at room temperature for 1 h. The cells were washed twice with PBS and incubated with Alexa Fluor 488-labeled anti-rabbit IgG (1:2000; Molecular Probes) in PBS containing 0.5% Triton X-100 at room temperature for 1 h. The coverslips were removed from wells and placed on slides using Prolong Anti-Fade mounting medium (Molecular Probes). The cells were visualized by indirect immunofluorescence at a magnification of 63× using an Axiovert 200 fluorescence microscope with an oil lens (Carl Zeiss, New York, NY).

Luciferase Assays—293T cells grown in 24-well plates were transfected with 0.18 μg/well of a reporter plasmid, which expresses firefly luciferase under either IRF-3/7 or NF-κB control (p-55C1BLuc or pNF-κB-Luc, respectively), and 0.02 μg/well of pRenilla-Luc, which expresses *Renilla* luciferase constitutively, using FuGENE 6 (Roche Applied Science) according to the manufacturer's instructions. 24 h following transfection, the cells were adsorbed with reovirus in serum-free medium at 4 °C for 1 h, followed by incubation at 37 °C in serum-containing medium for 24 h. For experiments using RIG-I plasmid constructs, the cells were transfected with 0.1 μg/well of plasmid expressing RIG-I mutants (vector, full-length RIG-I, RIG-IC (3), or RIG-IKA (3)), 0.09 μg/well of luciferase reporter, and 0.01 μg/well of pRenilla-luc. Alternatively, the cells were transfected with 5 μg/well of poly(I·C) (Amersham Biosciences) or reovirus genomic dsRNA (35) by calcium phosphate precipitation. Luciferase activity in the cultures was quantified using a dual luciferase assay kit (Promega, Madison, WI) according to the manufacturer's instructions.

RT-PCR—HeLa cells (10^5) grown in 24-well plates were either adsorbed with T3D at an MOI of 100 PFU/cell or mock infected in serum-free medium at 4 °C for 1 h, followed by incubation in serum-containing medium at 37 °C for various intervals. The cells were removed from plates with trypsin, washed once in PBS, and centrifuged at 500 × *g* for 5 min. The supernatant was removed, and the cell pellet was frozen at −70 °C. RNA was extracted using an RNEasy Mini RNA extraction kit (Qiagen) according to the manufacturer's instructions. RT-PCR was performed using the One-Step RT-PCR kit (Qiagen) and the following conditions: 0.5 μg of RNA template; 0.6 μM each primer; cycle for 30 min at 50 °C; 15 min at 95°; and 30 cycles of 1 min at 94 °C, 1 min at 55 °C, 1 min at 72 °C, followed by 10 min at 72 °C. RT-PCR products were resolved by electrophoresis in 2% Tris-borate-EDTA-agarose gels. Primer sequences are provided in the supplemental methods section.

Treatment with E64 or Ribavirin—After 24 h of incubation following transfection of 293T cells with luciferase reporter plasmids, the cells were either untreated or pretreated with 200 μM E64 (Sigma-Aldrich) for 4 h and adsorbed with either T3D virions or rsT3D-σ1T249I ISVPs at various MOIs in serum-free medium at 4 °C for 1 h. The cells were incubated at 37 °C for 24 h in the presence or absence of either 200 μM E64 or 200 μM ribavirin, and luciferase activity in cell culture lysates was quantified.

siRNA Transfections—For luciferase assays, 293T cells (10^6) were seeded into 60-mm tissue culture dishes (Costar) in medium without antibiotics and transfected with 266 pmol of siRNA using Lipofectamine 2000 reagent (Invitrogen) according to the manufacturer's instructions. After 24 h of incubation, the cells (7×10^4) were aliquoted into wells of 24-well plates in medium without antibiotics, incubated for 24 h, and transfected with 1 pmol/well of siRNA, 0.09 μg/well of firefly luciferase reporter plasmid, and 0.01 μg/well of pRenilla-Luc using Lipofectamine 2000. After 24 h of incubation, the cells were adsorbed with T3D in serum-free medium at an MOI of 100 PFU/cell at 4 °C for 1 h, followed by 24 h of incubation in serum-containing medium, at which time luciferase activity in cell culture lysates was determined. For caspase-3/7 assays, 24 h after the first siRNA transfection, cells (10^4) were transfected a second time by seeding into black clear-bottom 96-well plates (Costar) in antibiotic-free medium containing 5 pmol/well of siRNA and Lipofectamine 2000. After 24 h of incubation, the cells were adsorbed with T3D in serum-free medium at various MOIs at 4 °C for 1 h, followed by 24 h of incubation in serum-containing medium, at which time caspase-3/7 activity was determined.

Virus Growth—Cells (5×10^4) grown in 24-well plates were adsorbed in triplicate with T3D at various MOIs at 4 °C for 1 h in serum-free medium, washed once with PBS, and incubated in serum-containing medium for various intervals. To the indicated cultures, 200 and 800 IU of recombinant IFN-β was added at 12 and 24 h post-infection, respectively. The cells were frozen and thawed three times, followed by determination of viral titer/well by plaque assay using L929 cells (29). Viral yields were calculated according to the following formula: $\log_{10}\text{yield}_{t_x} = \log_{10}(\text{PFU/ml})_{t_x} - \log_{10}(\text{PFU/ml})_{t_0}$, where t_x is the time post-infection.

Quantitation of Apoptosis by Acridine Orange Staining—Cells (5×10^4) grown in the 24-well plates were infected with reovirus at various MOIs. The percentage of apoptotic cells after 48 h of incubation was determined using acridine orange staining as described (36). For each experiment, >200 cells were counted, and the percentage of cells exhibiting condensed chromatin was determined by epi-illumination fluorescence microscopy using a fluorescein filter set (Zeiss Photomicroscope III; Zeiss, New York).

Detection of Caspase-3/7 Activity—The cells (10^4) were seeded into black clear-bottom 96-well plates and adsorbed with T3D in serum-free medium at various MOIs at 4 °C for 1 h, followed by 24 h of incubation in serum-containing medium.

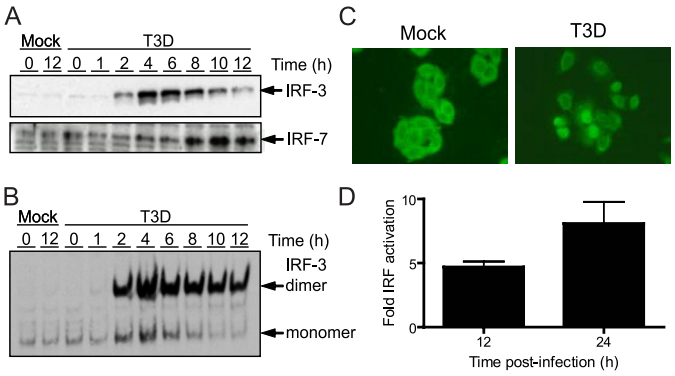

FIGURE 1. **Reovirus infection activates IRF-3 and IRF-7.** *A* and *B*, nuclear extracts were prepared from either mock infected HeLa cells (*Mock*) or cells infected with T3D at an MOI of 100 PFU/cell at the times shown. The extracts were resolved by SDS-PAGE (*A*) or native PAGE (*B*) and immunoblotted using an antiserum specific for IRF-3 (A, *top panel*) or IRF-7 (*A*, *bottom panel*). *C*, HeLa cells were either mock infected or infected with T3D at an MOI of 500 PFU/cell. At 8 h post-infection, the cells were fixed, stained with an antiserum specific for IRF-3 (*green*), and visualized by indirect immunofluorescence. *D*, 293T cells were co-transfected with p-55C1BLuc and pRenilla-Luc 24 h prior to infection with T3D at an MOI of 100 PFU/cell. Luciferase activity in cell lysates was determined at the indicated times post-infection. The results are presented as the ratios of normalized luciferase activity from infected cell lysates to that from mock infected lysates for triplicate samples. The *error bars* indicate S.D. *, $p < 0.05$ as determined by Student's *t* test in comparison with T3D.

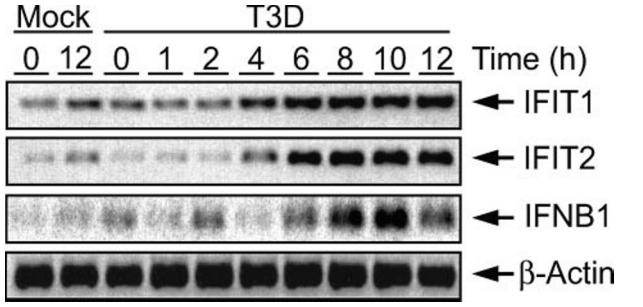

FIGURE 2. **Reovirus infection induces expression of IRF-3-dependent genes.** HeLa cells were infected with T3D at an MOI of 100 PFU/cell. RNA was extracted from infected cultures at the times shown and analyzed by one-step RT-PCR using primers specific for the indicated genes. Shown is a representative experiment of two performed.

Caspase-3/7 activity was quantified using the Caspase-Glo 3/7 assay system (Promega) according to the manufacturer's instructions.

RESULTS

To determine whether IRF-3 is activated following reovirus infection, we assayed for the presence of IRF-3 in nuclear extracts by immunoblotting (Fig. 1*A*) and for IRF-3 dimers by native PAGE (Fig. 1*B*) during a time course of reovirus T3D infection. Reovirus T3D activates NF-κB (20), stimulates IFN-β production (22), and induces apoptosis in cell culture (36) and in the murine central nervous system (18). In contrast to mock infected cells, T3D induced nuclear IRF-3 at 2 h post-infection, reached maximal levels at ~4–8 h, and decreased by 12 h. Concordantly, nuclear IRF-3 staining was observed in T3D-infected cultures but not in mock infected cultures at 8 h post-infection (Fig. 1*C*). The kinetics of reovirus-induced activation of IRF-3 parallel kinetics of NF-κB activation by reovirus (20, 33).

IRF-3 is expressed constitutively in most cell types and is activated initially following viral infection, whereas IRF-7 is transcriptionally up-regulated in response to IFN (12). To determine whether IRF-7 is activated by reovirus, we examined IRF-7 levels in nuclear extracts by immunoblotting over the same time course of reovirus T3D infection. IRF-7 was detected in nuclear extracts at 8–12 h post-infection, at the time when IRF-3 activation began to decline (Fig. 1*A*). This finding suggests that IRF-7 activity is induced following the initial activation of IRF-3 in reovirus-infected cells.

To determine whether reovirus infection stimulates functional IRF-3/7 activity, we used the p-55C1BLuc reporter plasmid (31), which expresses firefly luciferase under the control of tandem IRF-binding sites. Co-transfection of a plasmid constitutively expressing *Renilla* luciferase was used to normalize for transfection efficiency. T3D induced 5-fold higher levels of normalized luciferase activity in comparison with mock infection at 12 h post-infection and 8-fold higher levels at 24 h post-infection, indicating that T3D infection induces functional IRF-3/7 activity (Fig. 1*D*).

In addition to IFN-β, several genes are directly transcribed in response to IRF-3, including *IFIT1* (ISG56) and *IFIT2* (ISG54) (37). To determine whether those genes are up-regulated in reovirus-infected cells with kinetics that follow IRF-3 activation, we isolated RNA from HeLa cells over a time course of T3D infection and assayed for *IFIT1*, *IFIT2*, and *IFNB1* transcripts by RT-PCR (Fig. 2). *IFIT1* and *IFIT2* mRNAs were up-regulated in response to reovirus infection beginning ~4 h post-infection, with kinetics approximating those observed for IRF-3 activation. *IFNB1* was detected at 6–8 h post-infection, corresponding to the time of up-regulation of IRF-7. Collectively, these results indicate that reovirus strain T3D is a potent agonist of the IRF-3 transcriptional response.

Reovirus-induced NF-κB activation and apoptosis require virus disassembly in endosomes (30). To determine whether virus disassembly is required for IRF-3 activation, we tested the effect of E64, which inhibits endosomal cysteine proteases required for proteolytic cleavage of reovirus outer capsid proteins (38), on IRF-3/7 activation. E64 inhibited reovirus-induced IRF-3 activity but had no effect on IRF-3 activation by transfected poly(I·C) (Fig. 3*A*, *left panel*), indicating that disassembly of reovirus virions in endosomes is required for stimulation of IRF-3 activity. Similar results were obtained using the weak base ammonium chloride, which prevents endosomal acidification and virus disassembly (39) (supplemental Fig. S1). In contrast, E64 did not inhibit IRF-3 activation by reovirus ISVPs (Fig. 3*A*, *right panel*), which do not require endosomal acidification and proteolysis for penetration into the cytoplasm, indicating that E64 does not directly inhibit signaling pathways that activate IRF-3.

To determine whether the viral genome is required for IRF-3 activation by reovirus, we adsorbed 293T cells co-transfected with p-55C1BLuc and pRenilla-Luc with either viable (dsRNA+) or nonviable (dsRNA−) T3D particles. The latter were isolated as the "top component" of virions purified by cesium-chloride gradient centrifugation (28). Particles deficient in genomic dsRNA failed to activate IRF-3/7 by luciferase assay (Fig. 3*B*), suggesting that the viral genome is required for

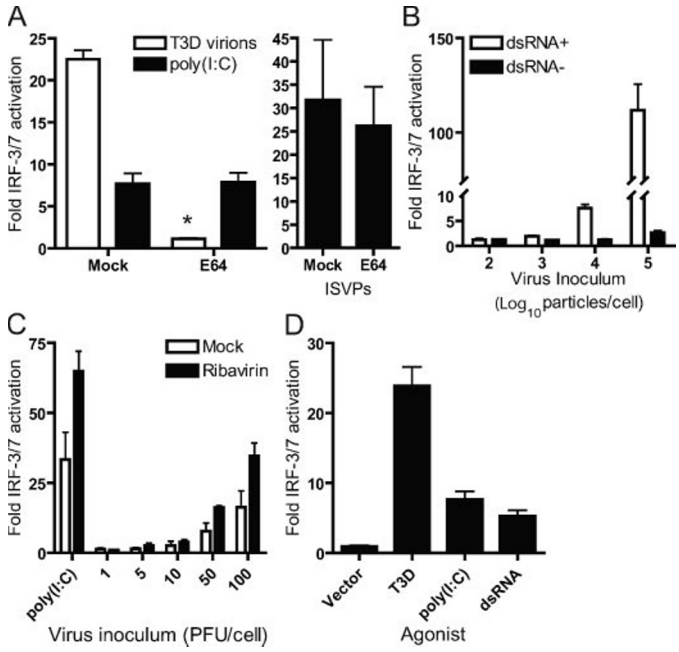

FIGURE 3. **Viral determinants of reovirus-induced IRF-3 activation.** 293T cells were co-transfected with p-55C1BLuc and pRenilla-Luc and incubated for 24 h. *A*, cells were treated with either PBS or 200 μM E64 for 4 h prior to infection with T3D (*left panel*) or rsT3D-σ1T249I ISVPs (*right panel*) at an MOI of 100 PFU/cell or transfection with poly(I·C). The cells were incubated in medium containing E64 for 24 h, at which time luciferase activity in cell culture lysates was determined. *B*, cells were incubated with either viable dsRNA-containing T3D virions (dsRNA+) or nonviable, genome-less T3D particles (dsRNA−) at the indicated concentrations. Luciferase activity in cell culture lysates was determined 24 h post-infection. *C*, cells were either infected with T3D at the indicated MOIs or transfected with poly(I·C) by the calcium phosphate method in the presence or absence of 200 μM ribavirin. Luciferase activity in cell culture lysates was determined at 24 h post-infection. *D*, cells were either infected with T3D at an MOI of 100 PFU/cell or transfected with DNA vector, poly(I·C), or reovirus genomic dsRNA isolated from purified virions. Luciferase activity in cell culture lysates was determined at 24 h post-infection or transfection. In all panels, the results are presented as the ratios of normalized luciferase activity from infected or transfected cell lysates to that from mock-treated lysates for triplicate samples. The *error bars* indicate S.D. *, $p < 0.05$ as determined by Student's *t* test in comparison with mock treatment.

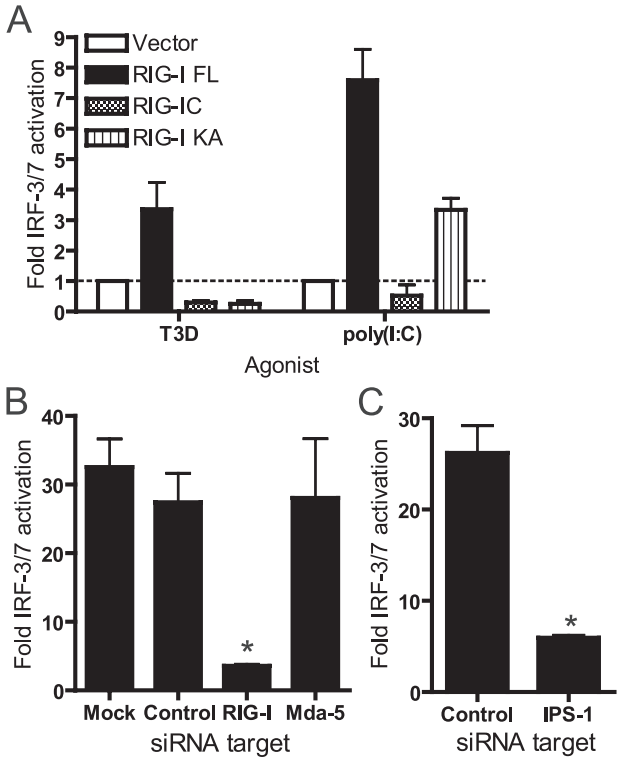

FIGURE 4. **Reovirus activates IRF-3 via RIG-I and IPS-1.** *A*, 293T cells were co-transfected with p-55C1BLuc, pRenilla-Luc, and with empty vector or plasmids expressing full-length RIG-I, RIG-IC, or RIG-IKA 24 h prior to infection with T3D at an MOI of 100 PFU/cell or transfection with poly(I·C) by the calcium phosphate method. Luciferase activity in cell culture lysates was determined at 24 h post-infection. The results are presented as the ratios of normalized luciferase activity from construct-expressing cell lysates to that from vector transfected cell lysates for each agonist, for triplicate samples. *B* and *C*, 293T cells were co-transfected with a control siRNA or an siRNA specific for either RIG-I (*B*), Mda-5 (*B*), or IPS-1 (*C*), and with p-55C1BLuc and pRenilla-Luc. Following 24 h incubation, the cells were infected with T3D at an MOI of 100 PFU/cell. Luciferase activity in cell culture lysates was determined at 24 h post-infection. In all panels, the results are presented as the ratios of normalized luciferase activity from infected cell lysates to that from mock infected lysates for triplicate samples. The *error bars* indicate S.D. *, $p < 0.05$ as determined by Student's *t* test in comparison with mock treatment.

induction of this response. However, treatment of cells with ribavirin, which blocks reovirus transcription (40), had no effect on IRF-3/7 activation induced by reovirus infection (Fig. 3*C*). This finding suggests that *de novo* viral RNA synthesis is not required for IRF-3 activation and that input genomic dsRNA is sufficient to activate this pathway. Transfection of purified genomic dsRNA activated IRF-3/7-dependent luciferase activity to an extent similar to poly(I·C), whereas transfection of DNA had no effect (Fig. 3*D*). We conclude that reovirus genomic dsRNA is necessary and sufficient to induce IRF-3 activity following reovirus infection.

We next examined the known signal transduction pathways linking cytoplasmic viral RNA to IRF-3. Two cytoplasmic RNA helicases, RIG-I and Mda-5, bind viral RNA and signal through the adaptor protein IPS-1 to activate Tank-binding kinase 1 and IKKε, kinases that phosphorylate IRF-3 (41). To determine whether these helicases are required for IRF-3 activation by reovirus, we used the dominant-negative inhibitors RIG-IC, which lacks the caspase activation and recruitment domain of RIG-I required for signaling to IPS-1 (3), and RIG-IKA, which contains a mutation in Walker's ATP-binding motif in the helicase domain (3). Transfection of full-length RIG-I enhanced IRF-3/7 activation following reovirus infection in comparison with transfection of empty vector. RIG-IC inhibited IRF-3/7 activity by both reovirus infection and poly(I·C) transfection (Fig. 4*A*), whereas RIG-IKA specifically inhibited IRF-3/7 activity by reovirus, but not by poly(I·C), suggesting involvement of RIG-I in the IRF-3/7 response evoked by reovirus.

To further discriminate between RIG-I and Mda-5 in reovirus-induced IRF-3 activation, we diminished expression of each protein individually using RNA interference. 293T cells were co-transfected with a control siRNA or siRNA specific for either RIG-I or Mda-5 prior to infection with T3D. Knockdown of *DDX58* (RIG-I) and *IFIH1* (Mda-5) mRNA levels was confirmed by RT-PCR (supplemental Fig. S2). Transfection of siRNA specific for RIG-I strongly inhibited IRF-3 activation by reovirus infection (Fig. 4*B*). In sharp contrast, siRNA specific for Mda-5 had no effect on reovirus-induced IRF-3 activity. Similar results were observed in experiments using HeLa cells (supplemental Fig. S3). Additionally, siRNA specific for RIG-I inhibited IRF-3/7 activity induced by transfection of reovirus genomic dsRNA (supplemental Fig. S4). These results indicate

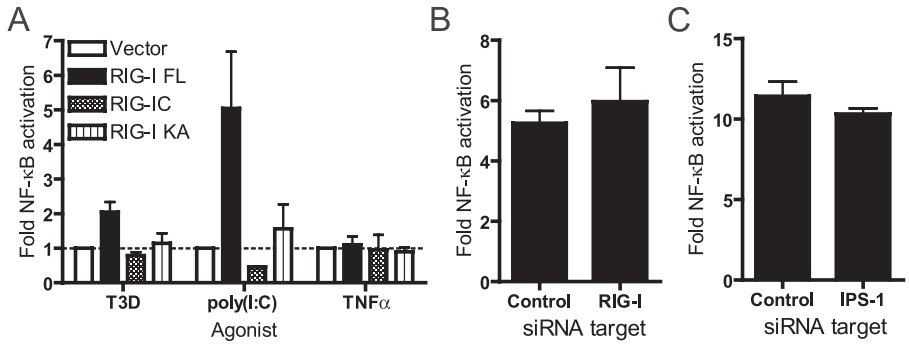

FIGURE 5. **Reovirus activates NF-κB independently of cytoplasmic sensors of viral RNA and IPS-1.** *A,* 293T cells were co-transfected with p-NF-κB-Luc, pRenilla-Luc, and with empty vector or plasmids expressing full-length RIG-I, RIG-IC, or RIG-IKA 24 h prior to infection with T3D at an MOI of 100 PFU/cell or transfection with 5 μg/ml poly(I·C) by the calcium phosphate method. 10 ng/ml tumor necrosis factor-α was added 8 h prior to harvest. Luciferase activity in cell culture lysates was determined at 24 h post-infection. The results are presented as the ratios of normalized luciferase activity from construct-expressing cell lysates to that from vector transfected cell lysates for each agonist, for triplicate samples. *B* and *C,* 293T cells were co-transfected with a control siRNA or an siRNA specific for either RIG-I (*B*) or IPS-1 (*C*), and with pNF-κB-Luc and pRenilla-Luc. Following 24 h of incubation, the cells were infected with T3D at an MOI of 100 PFU/cell. Luciferase activity in cell culture lysates was determined at 24 h post-infection. The results are presented as the ratios of normalized luciferase activity from infected cell lysates to that from mock-treated or mock infected lysates for triplicate samples. For all of the panels, the *error bars* indicate S.D. *, $p < 0.05$ as determined by Student's *t* test in comparison with mock treatment.

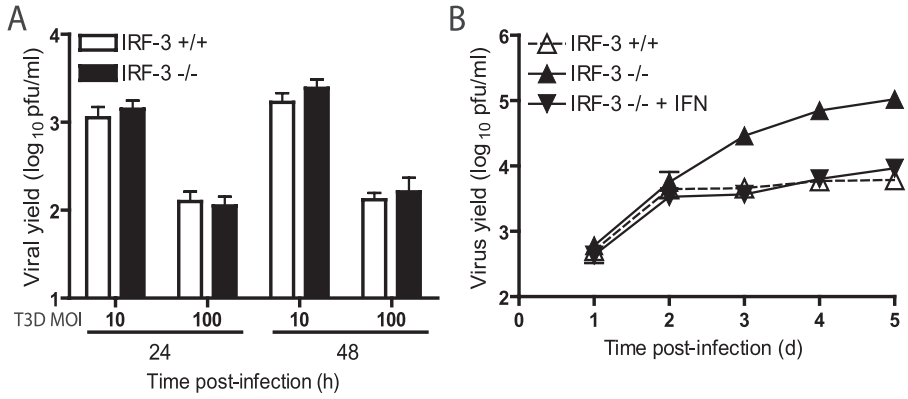

FIGURE 6. **Reovirus spread is diminished by IRF-3.** *A*, IRF-3 +/+ and IRF-3 −/− MEFs were infected with T3D at the indicated MOIs. Titers of infectious virus in cell lysates at 0, 24, and 48 h post-infection were determined by plaque assay. The results are expressed as viral yield for triplicate samples. The *error bars* indicate S.D. *B*, IRF-3 +/+ (△) and IRF-3 −/− MEFs (▲) were infected with T3D at an MOI of 1 PFU/cell. IRF-3 −/− MEFs were reconstituted with exogenous IFN-β at 12 and 24 h post-infection (▼). Titers of infectious virus at indicated times post-infection were determined by plaque assay. The results are expressed as viral yields for triplicate samples. The *error bars* indicate S.D.

that RIG-I is required for IRF-3/7 activation following reovirus infection.

To determine whether the RIG-I/Mda-5 adaptor protein IPS-1 is involved in reovirus-induced IRF-3 activation, we transfected 293T cells with siRNA specific for IPS-1 prior to reovirus infection. IPS-1 siRNA inhibited IRF-3 activation following reovirus infection by approximately the same magnitude as RIG-I siRNA (Fig. 4*C*). As expected, siRNA specific for IPS-1 also inhibited IRF-3 activation following transfection of poly(I·C) (supplemental Fig. S5). Together, these data indicate that reovirus activates IRF-3 via a pathway dependent on RIG-I and IPS-1.

RIG-I and IPS-1 activate both IRF-3 and NF-κB in response to cytoplasmic viral RNA (3, 7). To determine whether a signaling pathway involving RIG-I and IPS-1 is required for NF-κB activation by reovirus, we first tested RIG-IC for the capacity to alter NF-κB reporter gene activity following reovirus infection. Transfection of full-length RIG-I modestly increased NF-κB activation following reovirus infection (Fig. 5*A*). However, in contrast to IRF-3 activation, neither RIG-IC nor RIG-IKA inhibited reovirus-induced NF-κB activation. As positive and negative controls, respectively, RIG-IC blocked NF-κB activation by poly(I·C) but not that by tumor necrosis factor-α. In concordance with these data, an siRNA specific for either RIG-I or IPS-1 had no effect on NF-κB activation by reovirus (Fig. 5, *B* and *C*), but an siRNA specific for IPS-1 inhibited NF-κB activation by poly(I·C) (supplemental Fig. S5). As an additional control, reovirus-induced NF-κB activation was inhibited by a nonphosphorylatable, dominant-negative form of IκBα in the presence or absence of siRNA against IPS-1 (supplemental Fig. S6). These results indicate that reovirus activates NF-κB via a mechanism that is independent of RIG-I and IPS-1.

We next sought to determine the functional consequences of IRF-3 activation on reovirus infection. For these experiments, we used MEFs derived from animals genetically deficient in IRF-3 (25). We first characterized reovirus growth over a single cycle of viral replication following infection at an MOI of 10 and 100 PFU/cell, as determined by plaque titer on L-cells. Yields of T3D at 24 or 48 h post-infection following growth in IRF-3 +/+ or IRF-3 −/− MEFs did not differ (Fig. 6*A*). Thus, IRF-3 activation has little effect on reovirus growth during a single replication cycle. To determine whether IRF-3 limits the capacity of reovirus to spread in cell culture during multiple rounds of infection, we infected IRF-3 +/+ and IRF-3 −/− MEFs at an MOI of 1 PFU/cell and quantified titers over a time course of 5 days. At days 4 and 5 post-infection, reovirus reached 50-fold greater yields in IRF-3 −/− MEFs in comparison with those following infection of IRF-3 +/+ MEFs (Fig. 6*B*). Therefore, IRF-3 limits the capacity of reovirus to spread to uninfected cells in an infected culture.

To determine whether the capacity to produce IFN is correlated with diminished spread, we quantified IFN levels by enzyme-linked immunosorbent assay in supernatants of IRF-3 +/+ and IRF-3 −/− MEFs following T3D infection. As anticipated, IRF-3 was required for production of IFN-α and IFN-β following reovirus infection (supplemental Fig. S7, *A* and *B*, respectively). To confirm that the defect in IFN production was

responsible for the increase in virus growth observed in IRF-3 −/− MEFs, IRF-3 −/− MEFs were infected with T3D and reconstituted with exogenous recombinant IFN-β in the amount observed in IRF-3 +/+ MEFs infected with reovirus at 12 and 24 h post-infection (200 and 800 IU, respectively) (Fig. 6*B*). Exogenous addition of recombinant interferon limited reovirus growth in IRF-3 −/− MEFs to levels similar to those attained in IRF-3 +/+ MEFs, suggesting that the restriction of reovirus growth by IRF-3 is mediated by the production of type 1 IFNs.

The IFN network has been implicated in influencing the capacity of reovirus to induce apoptosis in cell culture (42) and *in vivo* (21). To determine the role of IRF-3 in reovirus-induced apoptosis, we examined the capacity of reovirus to induce apoptosis in IRF-3 +/+ and IRF-3 −/− MEFs. In comparison with IRF-3 +/+ MEFs, reovirus induced significantly lower levels of apoptosis in IRF-3 −/− MEFs as measured by caspase-3/7 activity in cell culture lysates (Fig. 7*A*) and acridine orange staining of infected cells (Fig. 7*B*). To assess the involvement of the RIG-I/IPS-1 signaling axis in apoptosis induced by reovirus, we examined the capacity of reovirus to induce caspase-3/7 activation in 293T cells transfected with siRNA specific for IPS-1. Caspase-3/7 activity induced by reovirus infection was reduced in cells transfected with an IPS-1 siRNA in comparison with those transfected with a control siRNA (Fig. 7*C*). Thus, pro-apoptotic signaling mediated by reovirus infection is enhanced by IPS-1 and IRF-3.

DISCUSSION

Innate immune detection of viral infection initiates signaling pathways that limit viral replication and diminish viral pathogenicity. Here, we demonstrate that viral genomic dsRNA initiates cellular responses via RIG-I, IPS-1, and IRF-3, which collectively function to enhance reovirus-induced apoptosis. Our data suggest that RIG-I is the primary sensor of reovirus infection in human 293T cells and HeLa cells. The efficient inhibition of IRF-3/7-dependent luciferase activity by siRNA directed against RIG-I suggests that Mda-5 cannot functionally compensate for RIG-I in detection of reovirus infection in these cells. Concordantly, the IFN response to reovirus is not attenuated in bone marrow-derived dendritic cells and macrophages from Mda-5 −/− mice (43). However, it is possible that other sensors function to recognize reovirus in some cell types. For example, reovirus induces IFN in Huh7.5 cells (44), a human hepatoma cell line in which RIG-I is defective (2).

RIG-I recognizes 5′ phosphates on single- or double-stranded RNA (5, 6). Reovirus (+)-strand RNAs are capped at the 5′ end (45), and therefore these RNAs would not be recognized as substrates by RIG-I. In contrast, reovirus (−)-strand RNAs bear an unblocked 5′ diphosphate (46), suggesting that the (−)-strand might serve as the reovirus RIG-I ligand. Reovirus (−)-strand synthesis is thought to occur within replicase particles (47), suggesting that (−)-strand RNAs would not have access to the cytosol where they could be engaged by RIG-I. However, it is possible that aberrant disassembly of reovirus particles in endosomes leads to proteolysis of the viral core and release of genomic dsRNA (containing both (+)- and (−)-strands) into the cytoplasm. Supporting this hypothesis, UV

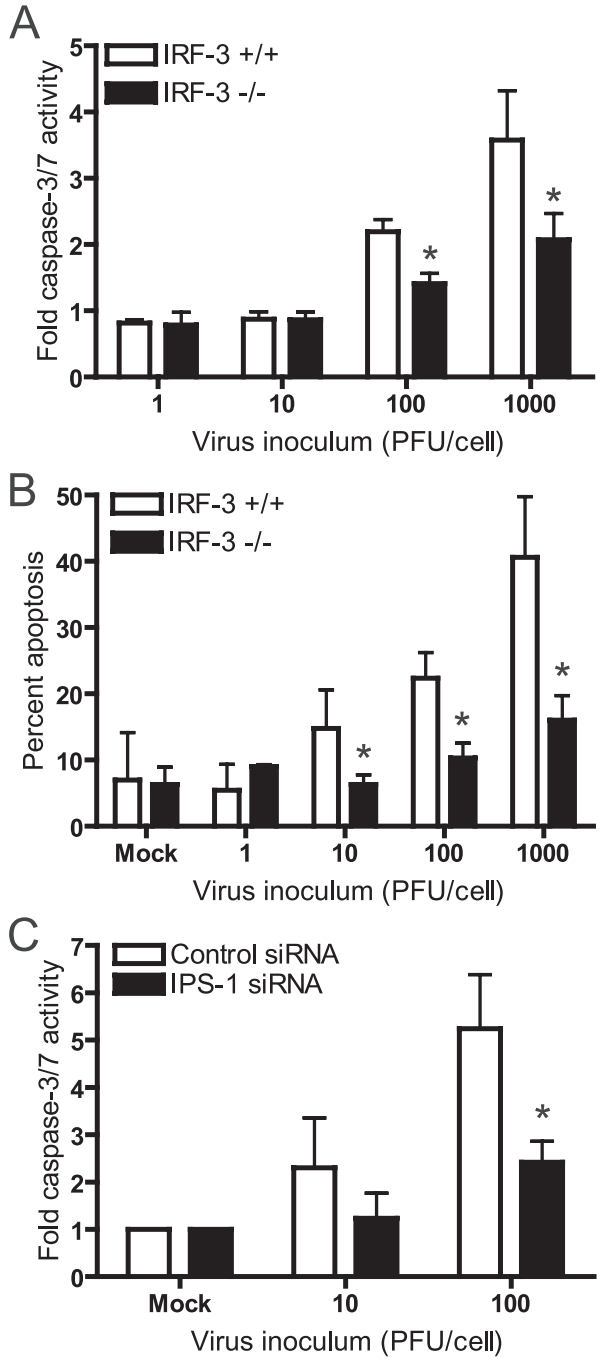

FIGURE 7. **IRF-3 is required for maximum induction of apoptosis by reovirus.** *A*, IRF-3 +/+ and IRF-3 −/− MEFs were infected with T3D at the indicated MOIs. Following 24 h of incubation, caspase-3/7 activity in cell lysates was determined. The results are expressed as the mean ratios of caspase-3/7 activity from infected cell lysates to that from mock infected cells for triplicate samples. The *error bars* indicate S.D. *, $p < 0.05$ as determined by Student's *t* test in comparison with IRF-3 +/+ MEFs at the same MOI. *B*, IRF-3 +/+ and IRF-3 −/− MEFs were infected with T3D at the indicated MOIs. Following 48 h of incubation, the percentage of apoptotic cells was determined after staining with acridine orange. The results are expressed as the mean percentages of apoptotic cells for triplicate samples. The *error bars* indicate S.D. *, $p < 0.05$ as determined by Student's *t* test in comparison with IRF-3 +/+ MEFs at the same MOI. *C*, 293T cells were transfected twice with a control siRNA or an siRNA specific for IPS-1. 24 h after the second transfection, the cells were infected with T3D at the indicated MOIs. Caspase-3/7 activity in cell lysates was determined 24 h post-infection. The results are expressed as the mean ratios of caspase-3/7 activity from infected cell lysates to that from mock infected cells for triplicate samples. The *error bars* indicate S.D. *, $p < 0.05$ as determined by Student's *t* test in comparison with cells transfected with the control siRNA at the same MOI.

treatment of reovirus virions enhances IFN production, suggesting that destabilizing the core may facilitate genomic dsRNA release (48). Alternatively, small RNA oligonucleotides associated with reovirus particles (49) may be released into the cytoplasm following viral disassembly where they could interact with RIG-I.

Other cellular sensors, including TLR3 (50) and PKR (51), respond to dsRNA and may function in antiviral signaling pathways initiated in response to reovirus infection. TLR3 is primarily expressed by conventional dendritic cells (52), a variety of epithelial cells (53), and astrocytes and microglia in the central nervous system (54). TLR3 binds to dsRNA that is internalized from the extracellular milieu into endosomes (50). Cell types used in this study, including 293T cells, express little detectable TLR3 (55), suggesting that TLR3 is not required for IFN production by reovirus. However, it is not known whether reovirus signals through TLR3 in cell types in which it is expressed. PKR responds to cytoplasmic dsRNA by phosphorylating eIF2α to inhibit protein synthesis (56). PKR is activated by reovirus and inhibits cellular protein synthesis following infection with certain strains of reovirus (57–59). However, as PKR is induced by IFN, these effects are likely mediated downstream of IFN release and thus would be secondary to the initial innate immune detection of reovirus.

NF-κB complexes containing p50 and RelA (p65) are activated following reovirus infection over a time course similar to the activation of IRF-3 (20, 33). NF-κB complexes activated by reovirus also contain c-Rel at 8 h post-infection and p52 at 20–24 h post-infection (33). Although other NF-κB family members are activated during reovirus infection, p50 and RelA are clearly required for reovirus-induced apoptosis (20), suggesting that the initial activation of NF-κB is essential for cell death signaling. Reovirus-induced NF-κB activation requires the α and γ subunits of the multi-component IKK complex (33), in contrast to the canonical activation of p50/Rel-A heterodimers, which requires IKKβ and IKKγ (60). The signal transducers that couple reovirus to the IKK complex are not known. Although engagement of RIG-I and IPS-1 activates NF-κB by some agonists (3, 7), we found that reovirus activates NF-κB independently of RIG-I and IPS-1. The reovirus μ1 protein is sufficient to induce apoptosis when expressed ectopically in cell culture (61), implicating μ1 in reovirus-induced NF-κB activation. We hypothesize that μ1 engages a cellular kinase that activates IKKα/IKKγ complexes or engages the IKKs directly to mediate NF-κB activation. Experiments are in progress to define mechanisms by which reovirus activates NF-κB.

Identification of IRF-3, in addition to NF-κB, as crucial signaling intermediaries in the cell death response to reovirus infection suggests several possible mechanisms by which these proteins direct an apoptotic program. One possibility is that these effects are mediated by the production of type I IFNs. Both IRF-3 and NF-κB, along with activating transcription factor-2/c-Jun, bind the IFN-β promoter and stimulate IFN-β production (1). Type I IFNs can be proapoptotic via the induction of proteins such as Fas and 2′,5′-oligoadenylate synthase, which direct apoptotic signaling (14, 62). IFN-β production in response to reovirus infection mediates a protective role in cardiac myocytes in culture and *in vivo* by inhibiting viral replication (21, 23). This effect may be due to rapid apoptosis of initially infected cells, thereby terminating viral replication at that site. An alternative possibility is that IRF-3- and NF-κB-mediated proapoptotic signaling is IFN-independent. Both transcription factors induce genes that have proapoptotic functions (37, 42, 63). For example, IRF-3 directly induces expression of tumor necrosis factor-related apoptosis-inducing ligand (64), which mediates reovirus-induced apoptosis in some cell types (65). The mechanism by which reovirus induces apoptosis also may be dependent on MOI. Our data suggest that at high MOI, IRF-3 has no effect on virus yield but enhances apoptosis, whereas at low MOI, IRF-3 limits reovirus spread. Therefore, we hypothesize that IRF-3 has a two distinct functions during reovirus infection; at high MOI, IRF-3 signaling triggers apoptosis, whereas at lower MOI, IRF-3 signaling induces type 1 IFNs to limit viral spread to surrounding cells. These differential effects may be due to the strength and duration of the IRF-3 signal.

IRF-3 activation by reovirus requires genomic dsRNA, RIG-I, and IPS-1. In contrast, RIG-I and IPS-1 are dispensable for reovirus-induced activation of NF-κB. Importantly, IRF-3 and IPS-1 are required for efficient induction of apoptosis following reovirus infection. To our knowledge, this is the first demonstration of the involvement of RIG-I and IPS-1 in cell death signaling in response to a virus. In the absence of IRF-3, reovirus-induced apoptosis is diminished, and viral replication is enhanced, suggesting that apoptosis serves as an antiviral host defense to limit reovirus infection. Because apoptosis is a hallmark of reovirus encephalitis (18) and myocarditis (19), findings in this report raise the possibility that similar mechanisms are used to effect reovirus-mediated tissue injury in the infected host. Moreover, these results define a new role for innate immune response sensors, solidifying evidence that apoptosis is an essential component of innate immunity.

Acknowledgments—We thank members of our laboratories for many helpful discussions and D. Ballard, N. Grandvaux, K. Mossman, G. Sen, and R. Siegel for providing reagents, advice, and comments.

REFERENCES

1. Mogensen, T. H., and Paludan, S. R. (2005) *J. Mol. Med.* **83,** 180–192
2. Sumpter, R. J., Loo, Y. M., Foy, E., Li, K., Yoneyama, M., Fujita, T., Lemon, S. M., and Gale, M. J. (2005) *J. Virol.* **79,** 2689–2699
3. Yoneyama, M., Kikuchi, M., Natsukawa, T., Shinobu, N., Imaizumi, T., Miyagishi, M., Taira, K., Akira, S., and Fujita, T. (2004) *Nat. Immunol.* **5,** 730–737
4. Kato, H., Takeuchi, O., Sato, S., Yoneyama, M., Yamamoto, M., Matsui, K., Uematsu, S., Jung, A., Kawai, T., Ishii, K. J., Yamaguchi, O., Otsu, K., Tsujimura, T., Koh, C. S., Reis e Sousa, C., Matsuura, Y., Fujita, T., and Akira, S. (2006) *Nature* **441,** 101–105
5. Hornung, V., Ellegast, J., Kim, S., Brzozka, K., Jung, A., Kato, H., Poeck, H., Akira, S., Conzelmann, K. K., Schlee, M., Endres, S., and Hartmann, G. (2006) *Science* **314,** 994–997
6. Pichlmair, A., Schulz, O., Tan, C. P., Naslund, T. I., Liljestrom, P., Weber, F., and Reis e Sousa, C. (2006) *Science* **314,** 997–1001
7. Kawai, T., Takahashi, K., Sato, S., Coban, C., Kumar, H., Kato, H., Ishii, K. J., Takeuchi, O., and Akira, S. (2005) *Nat. Immunol.* **6,** 981–988
8. Seth, R. B., Sun, L., Ea, C. K., and Chen, Z. J. (2005) *Cell* **122,** 669–682
9. Xu, L. G., Wang, Y. Y., Han, K. J., Li, L. Y., Zhai, Z., and Shu, H. B. (2005) *Mol. Cell* **19,** 727–740

10. Meylan, E., Curran, J., Hofmann, K., Moradpour, D., Binder, M., Bartenschlager, R., and Tschopp, J. (2005) *Nature* **437,** 1167–1172
11. Chawla-Sarkar, M., Lindner, D. J., Liu, Y. F., Williams, B. R., Sen, G. C., Silverman, R. H., and Borden, E. C. (2003) *Apoptosis* **8,** 237–249
12. Lu, R., Au, W. C., Yeow, W. S., Hageman, N., and Pitha, P. M. (2000) *J. Biol. Chem.* **275,** 31805–31812
13. Kayagaki, N., Yamaguchi, N., Nakayama, M., Eto, H., Okumura, K., and Yagita, H. (1999) *J. of Exp. Med.* **189,** 1451–1460
14. Selleri, C., Sato, T., Del Vecchio, L., Luciano, L., Barrett, A. J., Rotoli, B., Young, N. S., and Maciejewski, J. P. (1997) *Blood* **89,** 957–964
15. Heylbroeck, C., Balachandran, S., Servant, M. J., DeLuca, C., Barber, G. N., Lin, R., and Hiscott, J. (2000) *J. Virol.* **74,** 3781–3792
16. Nibert, M. L., and Schiff, L. A. (2001) in *Fields Virology* (Knipe, D. M., and Howley, P. M., eds) 4th Ed., pp. 1679–1728, Lippincott Williams & Wilkins, Philadelphia
17. Tyler, K. L. (2001) in *Fields Virology* (Knipe, D. M., and Howley, P. M., eds) 4th Ed., pp. 1729–1745, Lippincott Williams & Wilkins, Philadelphia
18. Oberhaus, S. M., Smith, R. L., Clayton, G. H., Dermody, T. S., and Tyler, K. L. (1997) *J. Virol.* **71,** 2100–2106
19. DeBiasi, R., Edelstein, C., Sherry, B., and Tyler, K. (2001) *J. Virol.* **75,** 351–361
20. Connolly, J. L., Rodgers, S. E., Clarke, P., Ballard, D. W., Kerr, L. D., Tyler, K. L., and Dermody, T. S. (2000) *J. Virol.* **74,** 2981–2989
21. O'Donnell, S. M., Hansberger, M. W., Connolly, J. L., Chappell, J. D., Watson, M. J., Pierce, J. M., Wetzel, J. D., Han, W., Barton, E. S., Forrest, J. C., Valyi-Nagy, T., Yull, F. E., Blackwell, T. S., Rottman, J. N., Sherry, B., and Dermody, T. S. (2005) *J. Clin. Investig.* **115,** 2341–2350
22. Sherry, B., Torres, J., and Blum, M. A. (1998) *J. Virol.* **72,** 1314–1323
23. Stewart, M. J., Smoak, K., Blum, M. A., and Sherry, B. (2005) *J. Virol.* **79,** 2979–2987
24. Noah, D. L., Blum, M. A., and Sherry, B. (1999) *J. Virol.* **73,** 10208–10213
25. Sato, M., Suemori, H., Hata, N., Asagiri, M., Ogasawara, K., Nakao, K., Nakaya, T., Katsuki, M., Noguchi, S., Tanaka, N., and Taniguchi, T. (2000) *Immunity* **13,** 539–548
26. Kobayashi, T., Antar, A. A. R., Boehme, K. W., Danthi, P., Eby, E. A., Guglielmi, K. M., Holm, G. H., Johnson, E. M., Maginnis, M. S., Naik, S., Skelton, W. B., Wetzel, J. D., Wilson, G. J., Chappell, J. D., and Dermody, T. S. (2007) *Cell Host Microbe* **1,** 147–157
27. Furlong, D. B., Nibert, M. L., and Fields, B. N. (1988) *J. Virol.* **62,** 246–256
28. Smith, R. E., Zweerink, H. J., and Joklik, W. K. (1969) *Virology* **39,** 791–810
29. Virgin, H. W., IV, Bassel-Duby, R., Fields, B. N., and Tyler, K. L. (1988) *J. Virol.* **62,** 4594–4604
30. Connolly, J. L., and Dermody, T. S. (2002) *J. Virol.* **76,** 1632–1641
31. Yoneyama, M., Suhara, W., Fukuhara, Y., Sato, M., Ozato, K., and Fujita, T. (1996) *J Biochem.* (*Tokyo*) **120,** 160–169
32. Carter, R. S., Geyer, B. C., Xie, M., Acevedo-Suarez, C. A., and Ballard, D. W. (2001) *J. Biol. Chem.* **276,** 24445–24448
33. Hansberger, M. W., Campbell, J. A., Danthi, P., Arrate, P., Pennington, K. N., Marcu, K. B., Ballard, D. W., and Dermody, T. S. (2007) *J. Virol.* **81,** 1360–1371
34. Iwamura, T., Yoneyama, M., Yamaguchi, K., Suhara, W., Mori, W., Shiota, K., Okabe, Y., Namiki, H., and Fujita, T. (2001) *Genes Cells* **6,** 375–388
35. Nibert, M. L., Dermody, T. S., and Fields, B. N. (1990) *J. Virol.* **64,** 2976–2989
36. Tyler, K. L., Squier, M. K., Rodgers, S. E., Schneider, S. E., Oberhaus, S. M., Grdina, T. A., Cohen, J. J., and Dermody, T. S. (1995) *J. Virol.* **69,** 6972–6979
37. Grandvaux, N., Servant, M. J., tenOever, B., Sen, G. C., Balachandran, S., Barber, G. N., Lin, R., and Hiscott, J. (2002) *J. Virol.* **76,** 5532–5539
38. Baer, G. S., and Dermody, T. S. (1997) *J. Virol.* **71,** 4921–4928
39. Sturzenbecker, L. J., Nibert, M. L., Furlong, D. B., and Fields, B. N. (1987) *J. Virol.* **61,** 2351–2361
40. Rankin, U. T., Jr., Eppes, S. B., Antczak, J. B., and Joklik, W. K. (1989) *Virology* **168,** 147–158
41. Sharma, S., tenOever, B. R., Grandvaux, N., Zhou, G. P., Lin, R., and Hiscott, J. (2003) *Science* **300,** 1148–1151
42. O'Donnell, S. M., Holm, G. H., Pierce, J. M., Tian, B., Watson, M. J., Chari, R. S., Ballard, D. W., Brasier, A. R., and Dermody, T. S. (2006) *J. Virol.* **80,** 1077–1086
43. Gitlin, L., Barchet, W., Gilfillan, S., Cella, M., Beutler, B., Flavell, R., Diamond, M., and Colonna, M. (2006) *Proc. Natl. Acad. Sci. U. S. A.* **103,** 8459–8464
44. Loo, Y.-M., Sumpter, R. J., Fredericksen, B. L., Foy, E., Yoneyama, M., Fujita, T., and Gale, M. J. (2005) in *American Society for Virology 24th Annual Meeting June 18–22*, University Park, PA
45. Furuichi, Y., Muthukrishnan, S., and Shatkin, A. J. (1975) *Proc. Natl. Acad. Sci. U. S. A.* **72,** 742–745
46. Banerjee, A. K., and Shatkin, A. J. (1971) *J. Mol. Biol.* **61,** 643–653
47. Morgan, E. M., and Zweerink, H. J. (1975) *Virology* **68,** 455–466
48. Henderson, D. R., and Joklik, W. K. (1978) *Virology* **91,** 389–406
49. Bellamy, A. R., and Joklik, W. K. (1967) *Proc. Natl. Acad. Sci. U. S. A.* **58,** 1389–1395
50. Alexopoulou, L., Holt, A. C., Medzhitov, R., and Flavell, R. A. (2001) *Nature* **413,** 732–738
51. Meurs, E., Chong, K., Galabru, J., Thomas, N. S., Kerr, I. M., Williams, B. R., and Hovanessian, A. G. (1990) *Cell* **62,** 379–390
52. Muzio, M., Bosisio, D., Polentarutti, N., D'amico, G., Stoppacciaro, A., Mancinelli, R., van't Veer, C., Penton-Rol, G., Ruco, L. P., Allavena, P., and Mantovani, A. (2000) *J. Immunol.* **164,** 5998–6004
53. Cario, E., and Podolsky, D. K. (2000) *Infect. Immunity* **68,** 7010–7017
54. Bsibsi, M., Ravid, R., Gveric, D., and van Noort, J. M. (2002) *J. Neuropath. Exp. Neurol.* **61,** 1013–1021
55. Matsumoto, M., Funami, K., Tanabe, M., Oshiumi, H., Shingai, M., Seto, Y., Yamamoto, A., and Seya, T. (2003) *J. Immunol.* **171,** 3154–3162
56. Clemens, M. J., and Elia, A. (1997) *J. Interferon Cytokine Res.* **17,** 503–524
57. Gupta, S. L., Holmes, S. L., and Mehra, L. L. (1982) *Virology* **12,** 495–499
58. Nilsen, T. W., Maroney, P. A., and Baglioni, C. (1982) *J. Biol. Chem.* **257,** 14593–14596
59. Smith, J. A., Schmechel, S. C., Williams, B. R., Silverman, R. H., and Schiff, L. A. (2005) *J. Virol.* **79,** 2240–2250
60. Li, Z. W., Chu, W., Hu, Y., Delhase, M., Deerinck, T., Ellisman, M., Johnson, R., and Karin, M. (1999) *J. Exp. Med.* **189,** 1839–1845
61. Coffey, C. M., Sheh, A., Kim, I. S., Chandran, K., Nibert, M. L., and Parker, J. S. (2006) *J. Virol.* **80,** 8422–8438
62. Castelli, J. C., Hassel, B. A., Wood, K. A., Li, X. L., Amemiya, K., Dalakas, M. C., Torrence, P. F., and Youle, R. J. (1997) *J. Exp. Med.* **186,** 967–972
63. Hayden, M. S., and Ghosh, S. (2004) *Genes Dev.* **18,** 2195–2224
64. Kirshner, J. R., Karpova, A. Y., Kops, M., and Howley, P. M. (2005) *J. Virol.* **79,** 9320–9324
65. Clarke, P., Meintzer, S. M., Gibson, S., Widmann, C., Garrington, T. P., Johnson, G. L., and Tyler, K. L. (2000) *J. Virol.* **74,** 8135–8139